

Received 13 March 2025, accepted 5 May 2025, date of publication 13 May 2025, date of current version 22 May 2025.

Digital Object Identifier 10.1109/ACCESS.2025.3569659

RESEARCH ARTICLE

Time-Dependent Analysis of the Interaction Between Energy Harvesting, Leakage, and Consumption Processes in a Green IoT Device

GODLOVE SUILA KUABAN¹, TADEUSZ CZACHÓRSKI¹, (Member, IEEE),
EROL GELENBE¹, (Life Fellow, IEEE), AND PIOTR CZEKALSKI²

¹Institute of Theoretical and Applied Informatics, Polish Academy of Sciences, 44-100 Gliwice, Poland

²Faculty of Automatic Control, Electronics and Computer Science, Silesian University of Technology, 44-100 Gliwice, Poland

Corresponding author: Godlove Suila Kuaban (gskuaban@iitis.pl)

This work was supported in part by the Reliable Electronics for Tomorrow's Active Systems (ReACTIVE Too) Project from European Union's Horizon 2020 Research, Innovation, and Staff Exchange Programme under the Marie Skłodowska-Curie Action under Grant 871163; in part by the International Project co-financed by the Program of the Minister of Science and Higher Education titled "Projekt Międzynarodowy Współfinansowany (PMW)" (2021–2025) under Contract 5169/H2020/2020/2; in part by the International Project, ReACTIVE Too co-financed by the Program of the Minister of Science and Higher Education titled "PMW" (2024–2025) under Contract 5872/H2020/2024/2; and in part by the Department of Computer Graphics, Vision, and Digital Systems under the Statutory Research Project (Rau6, 2025), Silesian University of Technology, Gliwice, Poland.

ABSTRACT The Internet of Things (IoT) is transforming industries by enhancing productivity and efficiency; however, energy availability remains a significant challenge due to the limited capacity of batteries and supercapacitors powering IoT devices. The emergence of Green IoT (G-IoT) frameworks, which prioritize energy efficiency and renewable energy integration, offers a promising solution to address this challenge. Despite these advancements, energy storage systems (ESSs) face issues such as capacity degradation, leakage, and charge redistribution, which can lead to energy depletion and service disruptions. Traditional models often assume constant energy harvesting rates, overlooking the time-varying nature of environmental conditions that influence energy availability. In this paper, we propose a novel mathematical framework that incorporates time-dependent fluctuations in the energy harvesting rate to analyse the dynamic interactions between energy harvesting, leakage, and consumption in green IoT systems. Our approach includes an Energy Packet Network (EPN) model to represent transient energy dynamics and a Markov model to capture fluctuations in the energy harvesting rate. Through numerical simulations, we evaluate the impact of key design parameters, such as ESS capacity, mean energy consumption rate, energy leakage, and energy harvesting rate variations, on critical performance metrics including the probability of energy depletion and the transient mean number of stored energy packets. The results highlight the importance of considering time-varying energy harvesting in the design and optimization of IoT systems for long-term operation and sustainability.

INDEX TERMS Time-dependent analysis, energy harvesting, energy leakage, energy-efficiency, green IoT.

I. INTRODUCTION

The Internet of Things (IoT) is one of the most transformative technologies of the 21st century, with applications spanning various industries, including transportation, energy, construction, agriculture, home automation, smart buildings, smart cities, environmental monitoring, healthcare, defense,

manufacturing, and logistics [1], [2]. The deployment of tens of billions of IoT devices is anticipated to drive productivity and efficiency across multiple sectors [3], solidifying IoT's role as a key enabler of Industry 4.0, which is reshaping modern industries.

Despite substantial progress in developing reliable and sustainable IoT systems, energy availability remains a fundamental challenge. IoT nodes are typically powered by batteries or supercapacitors, both of which have limited

The associate editor coordinating the review of this manuscript and approving it for publication was Mauro Fadda¹.

energy storage capacity [3], [4]. This limitation raises concerns about achieving long-term, uninterrupted operation of IoT devices, particularly those expected to function for several years without human intervention [5]. Moreover, energy storage systems (ESSs) are not ideal, and their inherent imperfections further restrict their performance. Key issues include capacity degradation over repeated charge-discharge cycles, energy leakage, and charge redistribution (notably in supercapacitors). These factors accelerate energy depletion, increasing the likelihood of energy-related service disruptions. A potential mitigation strategy is to incorporate these non-idealities into energy storage models to assess their impact accurately. However, this also adds complexity to the modeling process [6].

In recent years, substantial efforts have been made to enhance the energy reliability and sustainability of IoT systems. One of the key advancements in this domain is the Green IoT (G-IoT) framework [7], [8], [9], which focuses on optimizing energy efficiency, ensuring energy reliability, and integrating renewable energy sources. As the deployment of IoT devices scales into the tens of billions, adopting green IoT strategies is essential for minimizing carbon emissions, reducing electronic waste, and mitigating the environmental impact of IoT operations and disposal. A widely adopted approach in Green IoT is the implementation of energy-saving techniques to reduce power consumption. Several key strategies outlined in [7], [8], and [9] include duty cycling to reduce active power consumption, packet size reduction and transceiver optimization to minimize communication energy, energy-aware routing and adaptive sensing for efficient data collection, protocol overhead reduction to streamline communication, voltage and frequency scaling to optimize hardware power usage, energy-efficient hardware and software design, Green IoT communication technologies such as BLE, RFID, NFC, Zigbee, LoRa, and Sigfox, sustainable IoT architectures including green cloud computing, fog computing, and virtualization, as well as the use of sustainable materials and efficient energy management techniques such as energy thresholds. A comprehensive review of energy-saving methodologies for Green IoT is provided in [10], [11], and [12].

Energy Harvesting for Green IoT is another key strategy in green IoT, and it involves capturing energy from ambient or external renewable sources such as solar (photovoltaic), radio frequency (RF), wind, and mechanical vibrations. However, maintaining consistent energy availability remains a challenge due to the intermittent and unpredictable nature of these renewable sources [13]. Additionally, the energy harvested by IoT devices is often limited, typically in the range of a few hundred milliwatt-hours (mWh) or, in some cases, as low as a few hundred micro-watt-hours (μ Wh). This constraint underscores the importance of efficient energy management to maximize operational efficiency. A detailed review of various energy harvesting techniques for green IoT is provided in [1] and [12].

Designing energy-efficient IoT nodes requires careful consideration of energy leakage. Properly sizing energy harvesting and storage systems is essential to compensate for energy losses, thereby reducing the likelihood of service outages and prolonging the operational lifespan of the nodes. While many studies on IoT node energy performance [3], [14], [15], [16], [17], [18], [19], [20], [21], [22], [23] have not accounted for energy leakage in storage systems, some have specifically analysed its effects on wireless communication nodes [24], [25], [26], [27], [28], [29]. IoT systems are also often supported by computational and data storage servers, so that recent work has also considered the optimum allocation of tasks to multiple diverse processors as to optimize performance and minimize energy consumption of the system [30].

A novel technique for evaluating IoT energy performance—without focusing on the internal complexities of harvesters and storage systems—uses G-Network theory [31], a generalization of “product form” queueing networks, to include both the discrete work flow in a communication system, and the energy supply model in discrete units called energy packets, that was introduced in [14] and [15]. This approach employs queueing theory to represent the charging and discharging behaviour of ESS. Further exploration of this concept can be found in [16], [32], and [33].

Within this framework, energy harvested and stored in the battery is modelled as packet arrivals, whereas energy consumption is treated as packet servicing. Unlike traditional queueing models—where the service rate must exceed arrivals to prevent overload—an ESS must ensure a higher energy arrival rate than consumption to avoid depletion-induced service interruptions [24]. Another method characterizes energy variations within an ESS as a continuous stochastic process, such as fluid flow [17], [18], [19] or diffusion models [3], [21], [22], [23]. A major challenge when incorporating inefficiencies like leakage is that it introduces an additional deterministic or stochastic process that interacts with energy arrival and consumption dynamics. Moreover, since leakage is directly influenced by the ESS’s current energy level, it cannot be treated as an isolated factor but remains intrinsically linked to the energy storage and usage processes.

II. MAIN CONTRIBUTIONS OF THE PAPER

Most existing studies on the interaction between energy harvesting, leakage, and consumption processes, including those cited above, assume that the mean energy harvesting rate or the mean rate of energy packet delivery to the energy storage system remains constant. Consequently, these studies primarily rely on steady-state analysis. However, in real-world scenarios, energy harvesting is influenced by random and unpredictable environmental factors, making it inherently stochastic and time-varying.

A Markov process is commonly used to model fluctuations in the mean energy harvesting rate caused by changes in

weather conditions. In [34], [35], and [36], the authors employed a two-state Markov chain to represent the energy harvesting process, where one state corresponds to active energy harvesting, while the other represents periods with no harvested energy. Similarly, the authors in [28] and [37] proposed a four-state Markov model to capture weather state transitions, which, in turn, influence the energy harvesting rate over time.

Given the stochastic nature of energy harvesting, incorporating time-dependent variations in the harvesting rate into energy performance models is crucial for accurately evaluating the behaviour of energy storage systems (ESSs). Modelling the interplay between transient energy harvesting, leakage, and consumption processes provides valuable insights into the relationships between key design parameters—such as the energy capacity of the ESS, mean energy consumption rate, energy threshold, energy leakage parameter, and energy leakage model—and critical performance metrics, including the mean number of stored energy packets and the probability of complete energy depletion (energy service outage probability).

In this paper, we introduce a mathematical framework to analyse the dynamic interactions between time-dependent energy harvesting, leakage, and consumption processes in green IoT networks. Specifically, we propose:

- An energy packet model for the energy storage system that accounts for transient energy dynamics.
- A Markov model to characterize the time-dependent fluctuations in the mean energy harvesting rate.
- To validate our approach, we conduct numerical simulations to evaluate the impact of key design parameters.

We assess their effects on critical energy performance metrics, such as the transient mean number of stored energy packets and the probability of complete energy depletion.

III. DESCRIPTION OF THE MODEL

Consider a green IoT system comprising a sensor device, an energy storage system, and an energy harvesting system, as illustrated in Fig. 1. The system follows a harvest-store-consume energy configuration, meaning that the harvested energy is first stored and subsequently utilized for operation.

For analytical tractability, we model the energy packet arrival process to the storage system as a Poisson process, while the energy consumption process follows an exponential distribution. Although these assumptions may not always perfectly reflect real-world conditions, they serve as a first-order approximation, providing a tractable analytical framework. This allows for deeper insights into the dynamic interactions between energy harvesting, leakage, and consumption processes, facilitating performance evaluation and optimization of energy-efficient IoT systems.

A. ENERGY PACKET MODEL FOR THE ENERGY STORAGE SYSTEM

The discretization of energy into packets requires defining a quantization step, which corresponds to the size of an

energy packet. An energy packet, measured in mWh or mAh, represents a pulse of power or current over a specific time duration.

Since energy is primarily consumed during active periods—when the node performs sensing, computation, or communication—the energy packet size can be expressed as:

$$E_p = P_{\text{active}} \cdot t_{\text{active}}, \quad (1)$$

where P_{active} denotes the power consumed during active periods, and t_{active} represents the time of activity.

Although the quantization step can be arbitrarily chosen, consistency is required across energy harvesting, consumption, and storage processes.

Let C_B (in mWh) represent the capacity of the energy storage system (ESS), which could be a battery or supercapacitor. The total number of energy packets the ESS can store is given by:

$$B = \frac{C_B}{E_p}, \quad (2)$$

implying that the ESS can hold up to B discrete energy packets, with possible energy states $\{0, 1, 2, \dots, B\}$. We assume the IoT node remains in a dormant state and activates only when triggered by an external event, e.g. a system supervising a pipeline is awoken by the detection of a fluid leakage. We assume that such events are defined by the Poisson process. The time needed to consume an energy unit has the exponential distribution. These assumptions, while not universally precise, serve as a practical first-order approximation for analytical tractability.

The energy storage system's dynamics is modelled using an $M(t)/M(n)/1/B$ queueing system. In Kendall's notation [38], this corresponds to a system with exponentially distributed inter-arrival and service times, a single server, and finite storage capacity of B energy packets. The notation $M(n)$ accounts for a state-dependent service rate and $M(t)$ for time-dependent arrival rate.

Energy packet arrivals follow a Poisson process, implying exponentially distributed inter-arrival times with rate λ . The consumption time of an energy packet is also exponentially distributed, with rate $\mu(n)$, where n denotes the number of stored energy packets.

In an extended Markovian framework, phase-type distributions can replace the exponential assumption to better approximate real-world energy dynamics, though this increases the complexity by introducing additional states and imposes purely numerical solution.

The service rate $\mu(n)$, representing the inverse of the average service time, is given by:

$$\mu(n) = \mu_i + \theta(n), \quad (3)$$

where μ_i is the base energy consumption rate and $\theta(n)$ accounts for state-dependent energy leakage.

We assume that the consumption rate varies depending on the device's operational mode. When stored energy exceeds

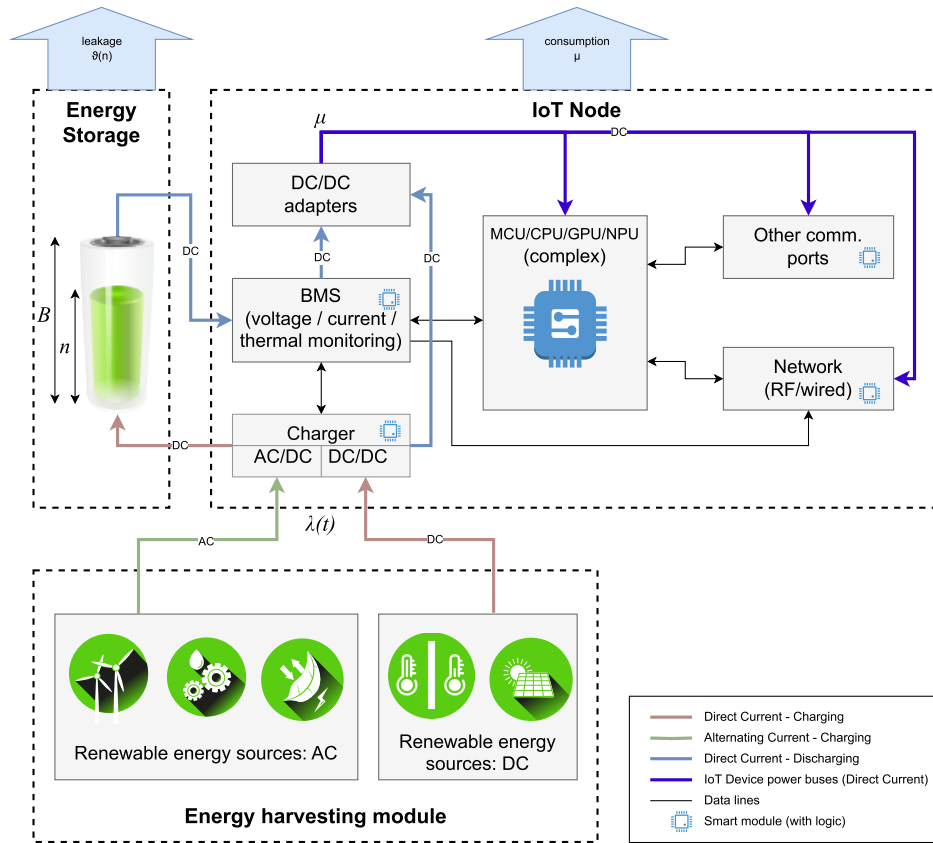


FIGURE 1. The architecture of a green IoT node with erratic energy sources such as radio frequency (RF), photovoltaic, thermal, wind, and mechanical vibration.

a threshold K ($n > K$), the system operates normally with $\mu_i = \mu_2$. If the energy level falls below K ($n \leq K$), the device switches to an energy-saving mode with $\mu_i = \mu_1$.

Three types of leakage rate functions $\theta(n)$ are considered:

- **linear leakage rate**, proportional to stored energy [24], [39]:

$$\vartheta(n) = (n - 1)\xi \quad (4)$$

- **exponential leakage rate** is exponentially related to the stored energy and is common in supercapacitors [28]:

$$\vartheta(n) = \alpha e^{\xi(n-1)}, \quad n \geq 1. \quad (5)$$

- **constant leakage rate**, independent of stored energy [26]:

$$\vartheta(n) = \alpha\xi. \quad (6)$$

This model provides a structured approach for analysing energy storage behaviour in IoT devices under varying conditions.

The evolution of energy packet levels in the ESS is modelled as an $M(t)/M(n)/1/B$ Markovian queueing process $\{N(t) \mid t \geq 0\}$. The probability of having n energy packets at time t is denoted as $p(n, t) = \Pr\{N(t) = n\}$.

The system dynamics are governed by the following first-order differential equations [40]:

$$\begin{aligned} \frac{dp(0, t)}{dt} &= -\lambda p(0, t) + \mu(1)p(1, t), \\ \frac{dp(n, t)}{dt} &= -(\lambda + \mu(n))p(n, t) + \lambda p(n - 1, t) \\ &\quad + \mu(n + 1)p(n + 1, t), \quad n = 1, \dots, B - 1, \quad (7) \end{aligned}$$

$$\frac{dp(B, t)}{dt} = \lambda p(B - 1, t) - \mu(B)p(B, t). \quad (8)$$

In the steady-state condition ($t \rightarrow \infty$), the system transitions to an equilibrium state where these differential equations reduce to algebraic equations [40]:

$$p(n) = p(0) \frac{\lambda^n}{\mu(1) \cdots \mu(n)}, \quad n = 1, \dots, B. \quad (9)$$

By enforcing the normalization condition $\sum_{n=0}^B p(n) = 1$, we obtain:

$$p(0) = \frac{1}{1 + \sum_{n=1}^B \left(\frac{\lambda^n}{\prod_{i=1}^n \mu(i)} \right)}. \quad (10)$$

This framework enables performance analysis of IoT energy storage systems under different operational constraints and event-driven consumption patterns.

B. TIME-DEPENDENT STOCHASTIC PROCESS FOR ENERGY HARVESTING

Since the energy harvested depends on random and unpredictable environmental variables, it exhibits a stochastic nature. The mean energy harvesting rate, denoted as λ , varies over discrete time intervals Δt . The evolution of λ can be modelled as either a random process or a Markov process.

Within each time interval Δt , λ is drawn from a predefined range $[\lambda_{\min}, \lambda_{\max}]$. In some simulations, λ is assumed to follow a uniform distribution, generating a new random value at each time step.

Alternatively, the time-dependent mean arrival rate of energy packets, $\lambda(t)$, can be modelled as a Markov process with N states and transition probabilities p_{ij} . The value of λ is influenced by dynamically changing environmental factors such as wind, sunlight, vibrations, cloud cover, and rainfall.

Consider a two-state Markov model that represents the environmental energy states S_0 and S_1 within each interval Δt . This type of model has been discussed in [34], [35], and [36]. The transition probabilities between the two states are p_{00} , p_{01} , p_{10} , and p_{11} , which can be estimated from empirical data [36]. The state transition matrix is given by:

$$P = \begin{bmatrix} p_{00} & p_{01} \\ p_{10} & p_{11} \end{bmatrix}$$

where:

- p_{00} is the probability of remaining in state S_0 ,
- p_{01} is the probability of transitioning from S_0 to S_1 ,
- p_{10} is the probability of transitioning from S_1 to S_0 ,
- p_{11} is the probability of remaining in state S_1 .

A more complex model can be defined using a three-state Markov chain (S_0, S_1, S_2) to represent different weather conditions such as sunny, cloudy, and rainy, which influence the state of a solar energy harvester. The corresponding values of λ for each state are $\lambda = \{\lambda_0, \lambda_1, \lambda_2\}$. A four-state weather model was explored in [28] and [37], where the state transition matrix is:

$$P = \begin{bmatrix} p_{00} & p_{01} & p_{02} & p_{03} \\ p_{10} & p_{11} & p_{12} & p_{13} \\ p_{20} & p_{21} & p_{22} & p_{23} \\ p_{30} & p_{31} & p_{32} & p_{33} \end{bmatrix}$$

Once the state transition matrix is defined, the Markov chain can be used to simulate dynamic state changes over time. The state at each time step determines the corresponding value of λ .

IV. TRANSIENT-STATE ENERGY PERFORMANCE ANALYSIS

We analyse the transient-state energy performance of the ESS with and without energy thresholds. While steady-state analysis assumes constant mean rates for energy packet delivery to and consumption from the ESS, the mean number of harvested energy packets can fluctuate over time.

We evaluate the impact of parameters such as energy leakage rate, energy harvesting rate, and the energy consumption rate on the energy performance metrics such as the service outage probability at time t , $p(0, t)$ and the mean number of energy packets present in the ESS at time t , $E[N(t)]$.

In the case of a single threshold and linear leakage rate, a simplified version of the differential equations in (8) can be obtained. Therefore, the following system of equations governs the time evolution of the state probabilities $p(0, t)$, $p(n, t)$, and $p(B, t)$, describing the dynamic behaviour of the system over time.

For $p(0, t)$ (empty state probability):

$$\frac{dp(0, t)}{dt} = -\lambda p(0, t) + \mu_1 p(1, t) \tag{11}$$

For intermediate states $p(n, t)$, where $1 \leq n \leq K - 1$:

$$\begin{aligned} \frac{dp(n, t)}{dt} = & -(\lambda + \mu_1 + (n - 1)\xi)p(n, t) \\ & + \lambda p(n - 1, t) + (\mu_1 + n\xi)p(n + 1, t) \end{aligned} \tag{12}$$

For intermediate states $p(n, t)$, where $K \leq n \leq B - 1$:

$$\begin{aligned} \frac{dp(n, t)}{dt} = & -(\lambda + \mu_2 + (n - 1)\xi)p(n, t) \\ & + \lambda p(n - 1, t) + (\mu_2 + n\xi)p(n + 1, t) \end{aligned} \tag{13}$$

For $p(B, t)$ (full state probability):

$$\frac{dp(B, t)}{dt} = \lambda p(B - 1, t) - (\mu_2 + (B - 1)\xi)p(B, t) \tag{14}$$

Initially, the system is assumed to be in state $p(0, 0)$, meaning all probabilities are zero except for $p(0, 0) = 1$, ensuring normalization.

The expected value of the number of energy packets in the ESS at time t , denoted as $E[N(t)]$ is the weighted sum of the probabilities of being at each state n , i.e.,

$$E[N(t)] = \sum_{n=0}^B np(n, t).$$

The transient solution of (8) is more intricate. It can be obtained using the Laplace transform, which converts the system's differential equations into algebraic equations in the Laplace domain. This transformation allows for an analytical solution, as demonstrated in [41]. However, this solution must be inverted numerically. Alternatively, a direct numerical approach can be used, as demonstrated here with our solver [42]. Many other solvers may be helpful.

The results presented in Figs. 2-12 are obtained by numerically solving the system described in equation 8. This is accomplished using Python libraries such as NumPy, SymPy, and SciPy.

First, we define λ as a time-dependent function, $\lambda(t)$, and implement a function to generate its values dynamically. The system of equations governing the time evolution of the number of EPs in the ESS is then formulated. After specifying the initial conditions—e.g., $p(0, 0) = 1$ if the ESS is empty

at $t = 0$ or $p(B, 0) = 0$ if the ESS initially contains B energy packets—SciPy is used to solve the system numerically.

To track the evolution of the mean number of energy packets in the ESS, we compute the expected value of the system at each time step. That is, at each time interval Δt , we obtain the value λ using a stochastic process. The computed values computed for each interval are then plotted using another Python library called Matplotlib.

To compute and plot the service outage probability, $p(0, t)$, we solve a system of differential equations that describe the dynamics of the queue of stored energy packets under time-varying arrival rates $\lambda(t)$.

Using a Markov chain, we generate a sequence of weather states that influence the evolution of $\lambda(t)$ over time. Each weather state corresponds to a distinct arrival rate $\lambda(t)$. The probability distribution $p(n, t)$ for different system states is governed by a set of coupled differential equations, which are solved using the `solve_ivp` function from SciPy.

Once the values of $p(0, t)$ are computed for each time interval Δt across various values of λ , they are visualized to analyse the system's performance.

Once the system is solved, $p(0, t)$ is plotted over time using a logarithmic scale. The results illustrate how $p(0, t)$ evolves under different service rate modification strategies. Additionally, the time-dependent arrival rate $\lambda(t)$ is overlaid on a secondary axis to highlight the impact of weather-induced variations in arrival intensity.

V. NUMERICAL SIMULATION RESULTS

In the presented numerical simulation results, we consider a battery with a charge rating of $Q = 2100$ mAh, a depth of discharge (DoD) of 70%, and a voltage of $v = 3.7$ V. The corresponding energy capacity of the battery is given by:

$$C_B = 2100 \times 0.7 \times 3.7 = 5439 \text{ mWh}$$

We assume that energy is quantized into discrete packets, with each packet having a size of $E_p = 54.39$ mWh. Consequently, the battery can store a maximum of:

$$B = \frac{5439}{54.39} = 100 \text{ energy packets}$$

For each numerical example, the relevant parameter values are provided alongside the corresponding figure.

The computational complexity of the numerical simulation primarily depends on the number of energy states B , the time resolution T , and the number of parameter variations. Specifically, the model solves a system of $B + 1$ coupled differential equations over T time steps for each value of the energy-efficiency parameter (e.g., ξ , μ , or κ), resulting in an overall time complexity of $\mathcal{O}(M \cdot B \cdot T)$, where M is the number of the parameter values simulated (number of simulations for each value of the parameter to generate a plot comparing influence of a given parameter).

Memory usage scales as $\mathcal{O}(B \cdot T)$, due to the need to store the full state probability distribution over time. Although

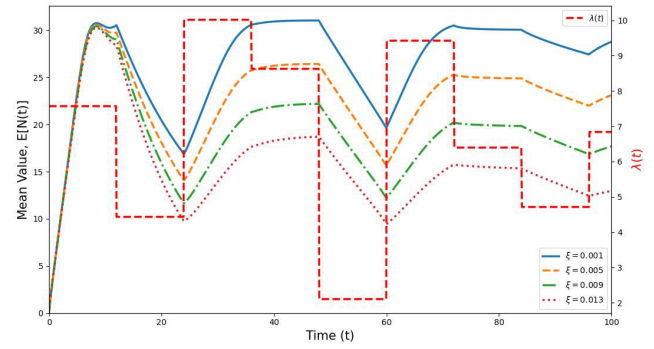


FIGURE 2. The evolution of $E[N(t)]$, for various values of ξ and randomly changing $\lambda(t)$: $\mu_2 = 5$, $\mu_1 = 3$, $K = 40$, $B = 100$.

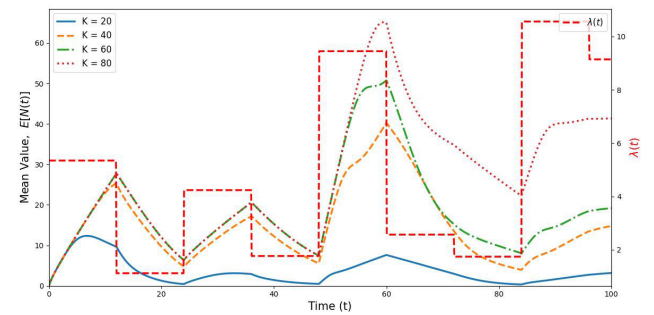


FIGURE 3. The evolution of $E[N(t)]$, for various values of K and randomly changing $\lambda(t)$: $\mu_2 = 5$, $\mu_1 = 3$, $\xi = 0.01$, $B = 100$.

computationally intensive, this approach remains tractable for moderate problem sizes and provides high-resolution insight into the energy dynamics of IoT systems under time-varying environmental conditions. However, increasing the state space or resolution (B or T) significantly raises the computational cost, especially if extended to parameter sweeps or Monte Carlo simulations. Thus, the computational complexity of this numerical computation is primarily determined by the dimensionality of the differential equation system, the resolution of the time vector, and the number of simulations for varying parameters.

A. THE IMPACT OF SYSTEM PARAMETERS ON THE MEAN NUMBER OF STORED ENERGY PACKETS

The mean number of stored energy packets is a key performance metric, as a higher number of stored packets allows the device to operate for a longer duration without depleting its energy reserves. If the stored energy is exhausted, the device will shut down.

We analyse the impact of model parameters such as λ , μ , ξ , and K on the mean number of stored energy packets. In each presented result, the values of $\lambda(t)$ are generated by a stochastic process that updates λ at regular or random time intervals Δt .

For Figs. 2 and 3, the values of $\lambda(t)$ are randomly generated using a uniform distribution with $\lambda_{\min} = 0$ and $\lambda_{\max} = 12$. The values of λ change every $\Delta t = 12$ hours. The remaining parameters are specified in the figures and their captions.

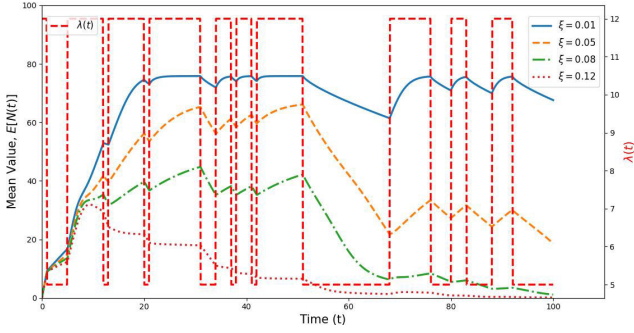


FIGURE 4. The evolution of $E[N(t)]$, for various values of ξ and $\lambda(t)$ from a weather Markov chain ($\lambda_{min} = 5$ and $\lambda_{max} = 12$): $\mu_2 = 5$, $\mu_1 = 3$, $K = 40$, $B = 100$.

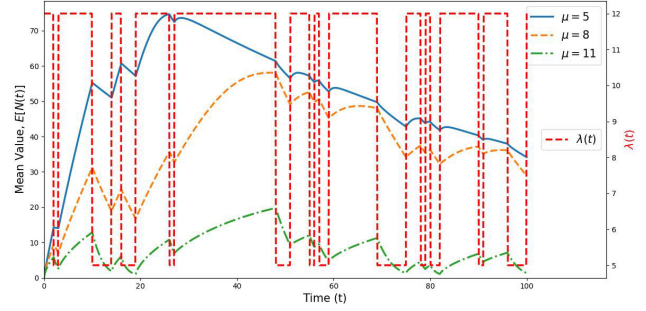


FIGURE 6. The evolution of $E[N(t)]$, for various values of μ , no energy threshold K , and $\lambda(t)$ from a weather Markov chain ($\lambda_{min} = 5$ and $\lambda_{max} = 18$): $\xi = 0.01$, $B = 100$.

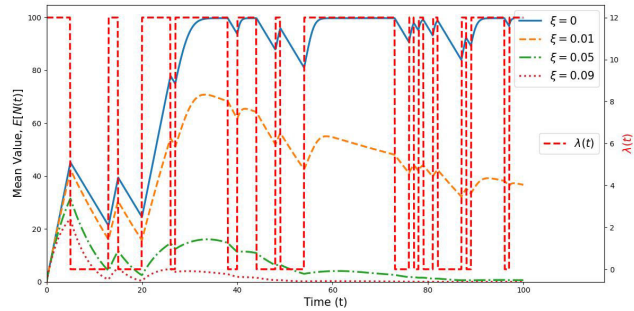


FIGURE 5. The evolution of $E[N(t)]$, for various values of ξ , no energy threshold K , and $\lambda(t)$ from a weather Markov chain ($\lambda_{min} = 5$ and $\lambda_{max} = 12$): $\mu_2 = 5$, $\mu_1 = 3$, $B = 100$.

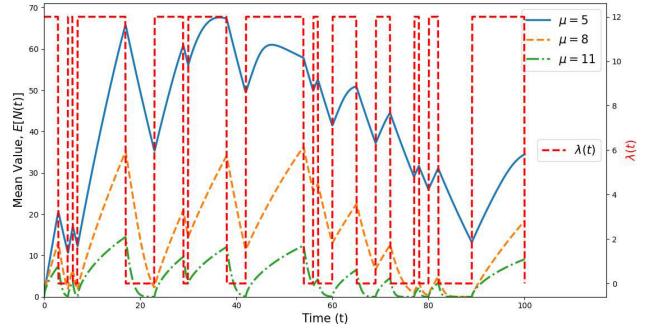


FIGURE 7. The evolution of $E[N(t)]$, for various values of μ , no energy threshold K , and $\lambda(t)$ from a weather Markov chain ($\lambda_{min} = 0$ and $\lambda_{max} = 18$): $\xi = 0.01$, $B = 100$.

Fig. 2 illustrates the evolution of $E[N(t)]$ for different values of ξ . In general, as the leakage parameter ξ increases, the mean number of energy packets (EPs) in the ESS decreases due to higher energy leakage. Fig. 3 shows the evolution of $E[N(t)]$ for various values of K . Higher values of the energy threshold K generally lead to an increase in the mean number of EPs in the ESS. This occurs because when the threshold is reached early—while sufficient energy remains in the ESS—the node enters energy-saving regimes sooner, slowing the depletion of stored EPs.

The time-dependent function $\lambda(t)$ can be derived from a weather Markov chain. We model the weather as a simple two-state Markov chain, where each state represents a different weather condition (e.g., sunny and rainy or sunny and not sunny). The state transitions determine the energy delivery rate $\lambda(t)$, which varies based on the current weather state.

When the weather state is S_0 , the mean energy delivery rate is λ_{max} , with a certain probability of transitioning to the S_1 state. Conversely, when the weather state is S_1 , the mean energy delivery rate is λ_{min} , with a probability of transitioning back to the S_0 state.

The transition matrix for this two-state Markov chain is given by:

$$P = \begin{bmatrix} 0.8 & 0.2 \\ 0.3 & 0.7 \end{bmatrix}$$

Fig. 4 shows the evolution of $E[N(t)]$ for various values of ξ , where $\lambda(t)$ is generated using the weather Markov chain with $\lambda_{min} = 5$ and $\lambda_{max} = 12$. The observed trend is consistent with that of Fig. 2, as discussed earlier. Also, Fig. 5 shows the evolution of $E[N(t)]$, for various values of ξ , without considering the energy threshold K , and the values of $\lambda(t)$ are generated from a weather Markov chain ($\lambda_{min} = 5$ and $\lambda_{max} = 12$). The trend is the same as in Figs. 2 and 4.

Since increasing or decreasing the energy harvesting rate can mitigate the impact of energy leakage, we analyse the influence of the mean energy harvesting rate and mean energy consumption rate on the evolution of the mean number of energy packets (EPs) in the ESS. Fig. 6 illustrates the evolution of $E[N(t)]$ for various values of μ , without considering the energy threshold K , where $\lambda(t)$ is generated using a weather Markov chain with $\lambda_{min} = 5$ and $\lambda_{max} = 12$. Similarly, Fig. 7 presents the evolution of $E[N(t)]$ under the same conditions, except that $\lambda(t)$ is generated from a weather Markov chain with $\lambda_{min} = 0$ and $\lambda_{max} = 12$.

In general, as the mean energy consumption rate μ increases, the mean number of EPs in the ESS decreases. This is expected, as higher values of μ lead to a faster depletion of stored EPs. The key difference between Fig. 6 and Fig. 7 is that in Fig. 7, the weather model allows for periods where no energy is harvested ($\lambda_{min} = 0$), which results in more pronounced fluctuations in $E[N(t)]$.

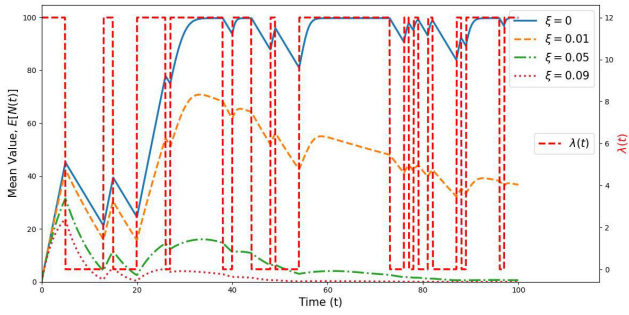


FIGURE 8. The evolution of $E[N(t)]$, for various values of ξ , no energy threshold K , and $\lambda(t)$ from a weather Markov chain: $\mu = 3$, $B = 100$.

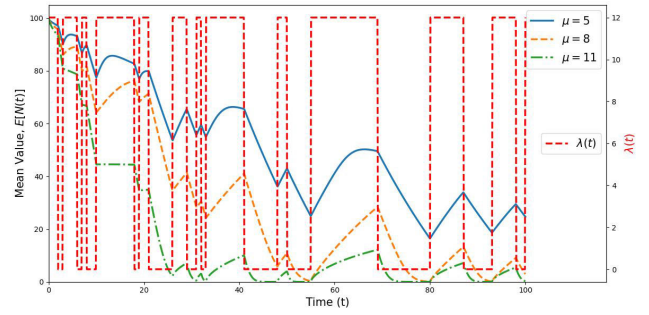


FIGURE 10. The evolution of $E[N(t)]$, for various values of μ , no energy threshold K , and $\lambda(t)$ from a weather Markov chain ($\lambda_{min} = 0$ and $\lambda_{max} = 12$): $\xi = 0.01$, $B = 100$, $p(B, 0) = 0$ (starting with B EPs in the ESS at $t = 0$).

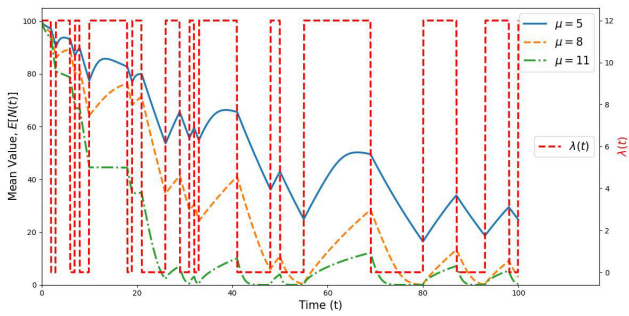


FIGURE 9. The evolution of $E[N(t)]$, for various values of μ , no energy threshold K , and $\lambda(t)$ from a weather Markov chain ($\lambda_{min} = 0$ and $\lambda_{max} = 12$): $\xi = 0.01$, $B = 100$, $p(B, 0) = 0$ (starting with B EPs in the ESS at $t = 0$).

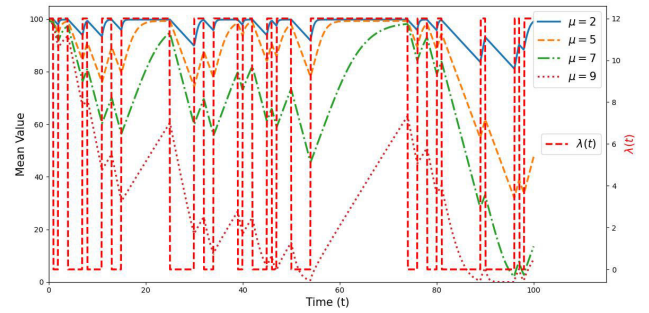


FIGURE 11. The evolution of $E[N(t)]$, for various values of μ , no energy threshold K , and $\lambda(t)$ from a weather Markov chain ($\lambda_{min} = 0$ and $\lambda_{max} = 12$): $\xi = 0.0$, $B = 100$, $p(B, 0) = 0$ (starting with B EPs in the ESS at $t = 0$).

Figure 8 depicts the evolution of $E[N(t)]$ for various values of ξ , excluding the impact of the energy threshold K . The energy arrival rate, $\lambda(t)$, is generated from a weather Markov chain. When $\xi = 0$, the energy storage system (ESS) is charged to full capacity, and the mean number of stored energy packets remains above 80% of its maximum capacity. As the energy leakage parameter ξ increases, the depletion rate of stored energy packets increases, leading to a rapid decline in energy packets in the ESS. For instance, when $\xi = 0.09$, the mean number of stored energy packets reaches zero before $t = 60$ time units. Conversely, lower values of ξ result in higher values of the mean number of energy packets over time. Since the leakage rate is an inherent characteristic of energy storage systems and beyond the control of an IoT system designer, mitigating its impact on the node's lifetime necessitates either reducing energy consumption or increasing energy harvesting rates.

The results presented in Figs. 2–8 assume that the energy storage system (ESS) initially contains zero energy packets (EPs) at time $t = 0$, i.e., $p(0, 0) = 1$. However, it is also possible to begin with B energy packets in the ESS at $t = 0$, represented as $p(B, 0) = 1$. The results shown in Figs. 9–12 are obtained under this assumption, meaning the system starts with B EPs at $t = 0$.

The observed trends regarding the influence of the mean energy consumption rate μ and the energy leakage parameter ξ remain consistent with those in Figs. 2–8. This consistency

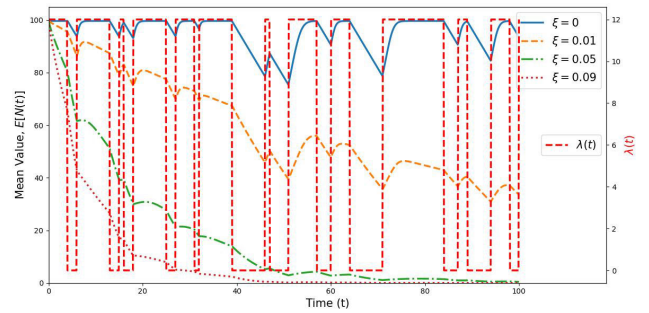


FIGURE 12. The evolution of $E[N(t)]$, for various values of ξ , no energy threshold K , and $\lambda(t)$ from a weather Markov chain ($\lambda_{min} = 0$ and $\lambda_{max} = 12$): $\mu = 3$, $B = 100$, $p(B, 0) = 0$ (starting with B EPs in the ESS at $t = 0$).

indicates that our proposed transient analysis framework is independent of the initial number of energy packets, whether it is zero or B at $t = 0$.

The mean energy delivery rate function, denoted as $\lambda(t)$, can be modelled using a Markov chain with any number of states. While previous examples considered a two-state Markov chain, we now extend the analysis to a four-state Markov chain, where each state corresponds to different weather conditions: Night (low or no energy), Sunny (high energy), Cloudy (medium energy), and Rainy (low to medium energy). Although this model focuses on solar energy, it can be generalized to incorporate multiple renewable energy

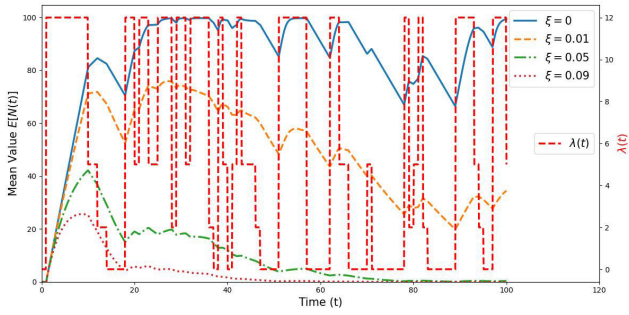


FIGURE 13. The evolution of $E[N(t)]$, for various values of ξ , no energy threshold K , and $\lambda(t)$ generated from a four state weather Markov chain: $\mu = 3, B = 100, p(0, 0) = 0$ (starting with $n = 0$ EPs in the ESS at $t = 0$).

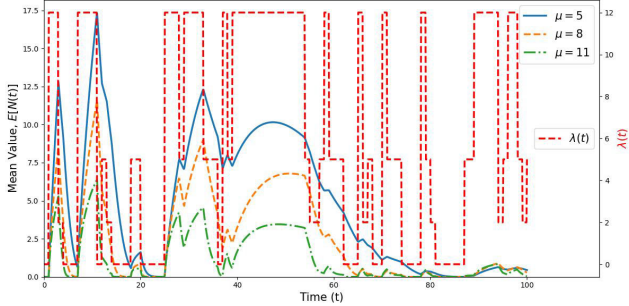


FIGURE 14. The evolution of $E[N(t)]$, for various values of μ , no energy threshold K , and $\lambda(t)$ generated from a four state weather Markov chain: $\xi = 0.05, B = 100, p(0, 0) = 0$ (starting with $n = 0$ EPs in the ESS at $t = 0$).

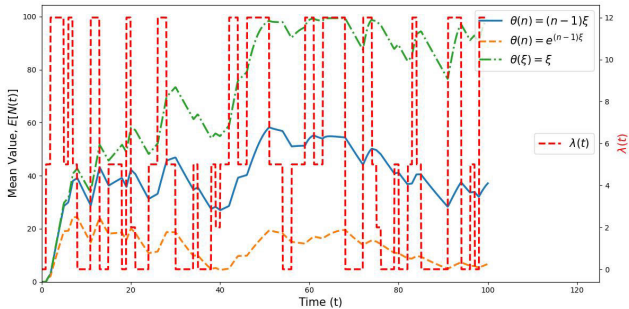


FIGURE 15. The evolution of $E[N(t)]$, for various energy leakage functions $\vartheta(n)$, no energy threshold K , and $\lambda(t)$ generated from a four state weather Markov chain: $\xi = 0.01, \mu = 3, B = 100, p(0, 0) = 0$ (starting with $n = 0$ EPs in the ESS at $t = 0$).

sources that fluctuate based on weather conditions. In such cases, the number of states could increase to better capture system complexities.

The authors in [43] studied the transient charging and discharging of a supercapacitor under varying transient energy harvesting rates, where the energy harvest rate $\lambda(t)$ fluctuates over time. Suppose that the values of $\lambda(t)$ are generated from a four-state Markov chain governed by the transition matrix:

$$P = \begin{bmatrix} 0.7 & 0.2 & 0.1 & 0.0 \\ 0.1 & 0.6 & 0.2 & 0.1 \\ 0.2 & 0.3 & 0.4 & 0.1 \\ 0.3 & 0.1 & 0.3 & 0.3 \end{bmatrix}$$

Figs. 13–15 illustrate the results obtained using the four-state Markov chain. Specifically, Fig. 13 examines the influence of the energy leakage parameter ξ on the evolution of the mean number of energy packets (EPs) in the energy storage system (ESS), while Fig. 14 investigates the impact of the energy consumption rate μ . The observed trends align with the findings from previous figures that analysed the effects of ξ and μ on the mean number of EPs in the ESS. A key aspect of these figures is the incorporation of a four-state Markov chain with four distinct values of $\lambda(t)$ (e.g., $\lambda = 0, 12, 5, 2$ corresponding to the states Night, Sunny, Cloudy, and Rainy, respectively).

Another significant result is shown in Fig. 15, which explores the impact of different energy leakage functions $\theta(n)$ on the evolution of the mean number of EPs in the ESS. Three energy leakage models are considered:

- **Linear energy leakage:** $\theta(n) = (n - 1)\xi$
- **Exponential energy leakage:** $\theta(n) = e^{(n-1)\xi}$
- **Constant energy leakage:** $\theta(n) = \xi$

The results indicate that the exponential energy leakage model performs the worst, followed by the linear model. This is because, in the exponential energy leakage model, the energy leakage rate grows exponentially with the number of EPs remaining in the ESS, whereas in the linear model, the leakage rate increases linearly. Experimental studies have demonstrated that energy leakage in supercapacitors often follows an exponential model [44], [45], [46].

B. THE IMPACT OF SYSTEM PARAMETERS ON THE SERVICE OUTAGE PROBABILITY

In this section, we compute the transient probability of service outage, which quantifies the likelihood of complete energy depletion in the system. Reducing the service outage probability is essential to ensure continuous operation and prevent disruptions caused by the shutdown of the IoT node due to insufficient stored energy.

Following the approach used in the numerical simulations for the transient mean number of stored energy packets, we investigate how key model parameters— λ, μ, ξ , and K —influence system performance.

Figures 16-20 illustrate the evolution of the transient probability of depleting all stored energy packets. These results are obtained using the four-state Markov chain representing weather conditions, which was previously employed in the numerical simulations of the transient mean number of stored energy packets. All other relevant parameters are provided in the figure captions.

In the simulations of $p(0, t)$, we assume $B = K$, meaning that the mean energy consumption rate, μ , remains constant.

The general trend observed is that the transient probability of energy depletion, $p(0, t)$, varies dynamically with changes in the mean energy delivery rate, $\lambda(t)$. If the initial number of stored energy packets is $n = 0$ at $t = 0$, then $p(0, 0) = 1$, and $p(0, t)$ evolves according to variations in $\lambda(t)$. Conversely, if the system starts with $n = B$ energy packets at $t = 0$,

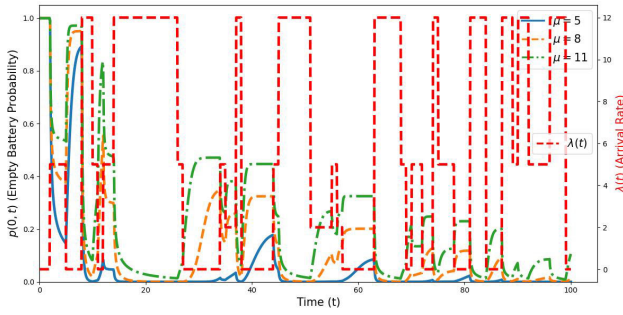


FIGURE 16. The evolution of $p(0, t)$, for various energy consumption rate μ , no energy threshold K , and $\lambda(t)$ generated from a four state weather Markov chain: $\xi = 0.01$, $B = 100$, $p(0, 0) = 1$ (starting with $n = 0$ EPs in the ESS at $t = 0$).

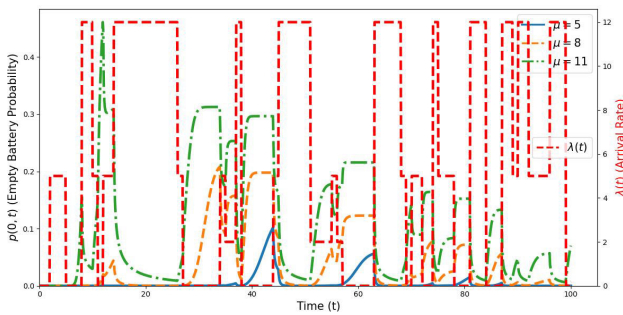


FIGURE 17. The evolution of $p(0, t)$, for various energy consumption rate μ , no energy threshold K , and $\lambda(t)$ generated from a four state weather Markov chain: $\xi = 0.05$, $B = 100$, $p(B, 0) = 1$ (starting with $n = B$ EPs in the ESS at $t = 0$).

then $p(0, 0) = 0$, and $p(0, t)$ increases dynamically based on the fluctuations in $\lambda(t)$.

In the simulations, the mean energy consumption rate is set to $\mu = \{5, 8, 11\}$. The values of λ corresponding to the energy states S_0, S_1, S_2 , and S_3 are given by: $\lambda = \{0, 12, 5, 2\}$ with the corresponding state transition probability matrix:

$$P = \begin{bmatrix} 0.7 & 0.2 & 0.1 & 0.0 \\ 0.1 & 0.6 & 0.2 & 0.1 \\ 0.2 & 0.3 & 0.4 & 0.1 \\ 0.3 & 0.1 & 0.3 & 0.3 \end{bmatrix}$$

It is observed that when the mean energy harvesting rate, λ , decreases from higher to lower values, the probability of energy depletion at time t increases, and vice versa.

Figures 16 and 17 show the influence of the mean energy consumption rate, μ , on $p(0, t)$. The results indicate that the probability of depleting all stored energy packets increases significantly with higher energy consumption rates. This increase is particularly pronounced during time intervals when the mean harvesting rate, λ , is lower than the mean consumption rate, μ . The key difference between Figures 16 and 17 is the initial energy level: in Figure 16, the system starts with $n = 0$ at $t = 0$, whereas in Figure 17, it starts with $n = B$.

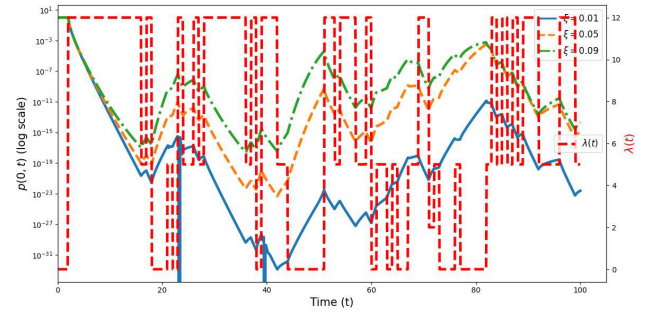


FIGURE 18. The evolution of $p(0, t)$, for various leakage parameter ξ , no energy threshold K , and $\lambda(t)$ generated from a four state weather Markov chain: $\mu = 3$, $B = 100$, $p(0, 0) = 1$ (starting with $n = 0$ EPs in the ESS at $t = 0$).

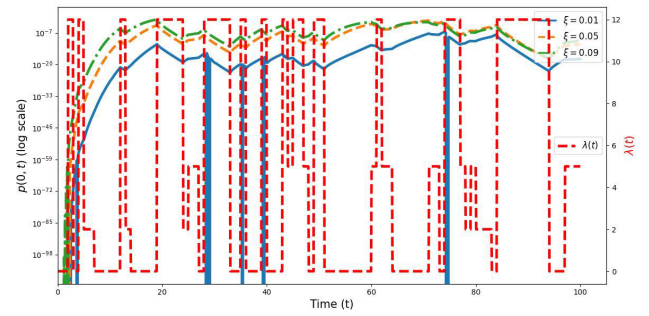


FIGURE 19. The evolution of $p(0, t)$, for various leakage parameter ξ , no energy threshold K , and $\lambda(t)$ generated from a four state weather Markov chain: $\mu = 3$, $B = 100$, $p(B, 0) = 1$ (starting with $n = B$ EPs in the ESS at $t = 0$).

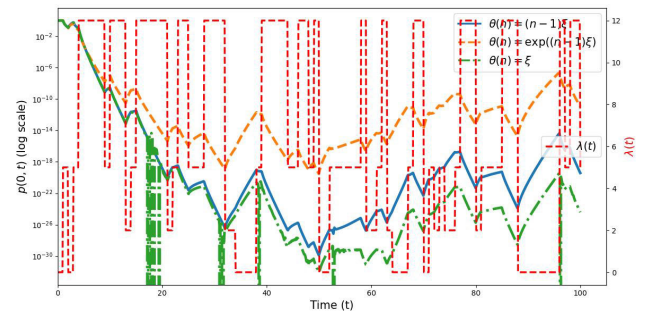


FIGURE 20. The evolution of $p(0, t)$, for various energy leakage functions $\vartheta(n)$, no energy threshold K , and $\lambda(t)$ generated from a four state weather Markov chain: $\xi = 0.01$, $\mu = 3$, $B = 100$, $p(0, 0) = 0$ (starting with $n = 0$ EPs in the ESS at $t = 0$).

Figures 18-20 illustrate the impact of the energy leakage rate on the probability of depleting all stored energy packets. Specifically, Figures 18-19 show the influence of the energy leakage parameter ξ on $p(0, t)$. The general trend indicates that as ξ increases, the probability of energy depletion also increases.

The key difference between the results in Figures 18 and 19 lies in the initial energy levels. In Figure 18, the system starts with $n = 0$ at $t = 0$, meaning there is no energy packet in the energy storage system (ESS) initially. In contrast, Figure 19 assumes $n = B$ at $t = 0$, meaning the ESS starts with B stored

energy packets. Additionally, in Figure 19, the values of $p(0, t)$ are displayed on a logarithmic scale to better observe very small probabilities. This is necessary because starting with $n = B$ energy packets at $t = 0$ results in extremely low values of $p(0, t)$.

The results in Figures 16-19 are computed using the linear energy leakage model. In Figure 20, we analyse the effect of different energy leakage models on $p(0, t)$. The highest values of $p(0, t)$ are observed with the exponential leakage model, followed by the linear leakage model, and finally, the constant leakage model, which results in the lowest values of $p(0, t)$. This occurs because, in the exponential leakage model, the energy leakage rate increases exponentially with the number of stored energy packets. Consequently, the constant leakage model exhibits the lowest probability of service outage, followed by the linear leakage model, and finally, the exponential leakage model, which results in the highest service outage probability.

VI. CONCLUSION

In this paper, we introduced a novel mathematical framework to analyse the dynamic interactions between time-dependent energy harvesting, leakage, and consumption processes in green IoT networks. By incorporating transient energy dynamics and utilizing a Markov model to capture fluctuations in the energy harvesting rate, we were able to provide a more accurate representation of the challenges faced by IoT devices in real-world environments. Through our numerical simulations, we demonstrated the significant impact of key design parameters, such as energy storage system capacity, mean energy consumption rate, energy leakage, and variations in energy harvesting rates, on critical performance metrics like the probability of energy depletion and the transient mean number of stored energy packets. Our findings emphasize the necessity of accounting for time-varying energy harvesting rates and non-idealities in energy storage systems to enhance the reliability and sustainability of green IoT systems.

Frequent fluctuations in renewable energy sources can significantly affect the availability of IoT nodes—manifesting as increased outage probability and reduced operational lifetime—particularly for energy-intensive devices with limited storage capacity. Such variability can lead to recurring energy-related disruptions, compromising the reliability and continuity of IoT system performance. Therefore, when designing renewable energy systems for IoT applications, it is essential for system designers to account for the stochastic and time-varying nature of renewable energy sources. Additionally, they must consider the effects of energy leakage from storage systems and incorporate a reasonable safety margin in the energy harvesting output to ensure long-term, uninterrupted operation—ideally enabling the IoT node to function reliably for several years without energy-related failures.

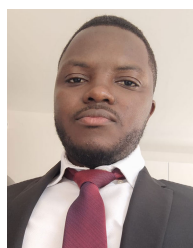
The primary limitation of the proposed framework lies in its assumption that the time interval between successive

energy packet deliveries to the energy storage system (ESS) follows a Poisson process, and that the time required to consume an energy packet is exponentially distributed. While these assumptions may not fully capture real-world dynamics, they offer a practical first-order approximation that facilitates analytical tractability and provide practical insights on the time-dependent behaviour of energy storage systems supplied by time-dependent energy sources. In future work, we aim to enhance the model by employing diffusion approximation, fluid flow approximation, and other numerical simulation techniques that do not rely on specific distributional assumptions for energy delivery and consumption processes. Additionally, we will focus on refining the existing models and investigating optimization strategies to improve energy efficiency, particularly in resource-constrained IoT environments.

REFERENCES

- [1] T. Sanislav, G. D. Mois, S. Zeadally, and S. C. Folea, "Energy harvesting techniques for Internet of Things (IoT)," *IEEE Access*, vol. 9, pp. 39530–39549, 2021.
- [2] Y. Santo, A. Abelém, A. Riker, and E. E. Tsiropoulou, "Integrating data privacy and energy management in smart cities with partial sustainable IoT networks," *IEEE Access*, vol. 13, pp. 33176–33188, 2025.
- [3] G. S. Kuaban, E. Gelenbe, T. Czachórski, P. Czekalski, and J. K. Tangka, "Modelling of the energy depletion process and battery depletion attacks for battery-powered Internet of Things (IoT) devices," *Sensors*, vol. 23, no. 13, p. 6183, Jul. 2023.
- [4] O. Alamu, T. O. Olwal, and E. M. Migabo, "Machine learning applications in energy harvesting Internet of Things networks: A review," *IEEE Access*, vol. 13, pp. 4235–4266, 2025.
- [5] G. Moloudian, M. Hosseinifard, S. Kumar, R. B. V. B. Simorangkir, J. L. Buckley, C. Song, G. Fantoni, and B. O'Flynn, "RF energy harvesting techniques for battery-less wireless sensing, industry 4.0, and Internet of Things: A review," *IEEE Sensors J.*, vol. 24, no. 5, pp. 5732–5745, Mar. 2024.
- [6] G. S. Kuaban, T. Czachórski, E. Gelenbe, P. Pecka, V. Nkemeni, and P. Czekalski, "Impact of energy leakage on the energy performance of green IoT nodes," in *Proc. 32nd Int. Conf. Modeling, Anal. Simulation Comput. Telecommun. Syst. (MASCOTS)*, Oct. 2024, pp. 1–8.
- [7] A. Al-Ansi, A. M. Al-Ansi, A. Muthanna, I. A. Elgandy, and A. Koucheryavy, "Survey on intelligence edge computing in 6G: Characteristics, challenges, potential use cases, and market drivers," *Future Internet*, vol. 13, no. 5, p. 118, Apr. 2021.
- [8] K. Sadatdiyov, L. Cui, L. Zhang, J. Z. Huang, S. Salloum, and M. S. Mahmud, "A review of optimization methods for computation offloading in edge computing networks," *Digit. Commun. Netw.*, vol. 9, no. 2, pp. 450–461, Apr. 2023.
- [9] M. H. Alsharif, A. Jahid, A. H. Kelechi, and R. Kannadasan, "Green IoT: A review and future research directions," *Symmetry*, vol. 15, no. 3, p. 757, Mar. 2023.
- [10] M. A. Albreem, A. M. Sheikh, M. H. Alsharif, M. Jusoh, and M. N. M. Yasin, "Green Internet of Things (GIoT): Applications, practices, awareness, and challenges," *IEEE Access*, vol. 9, pp. 38833–38858, 2021.
- [11] R. Arshad, S. Zahoor, M. A. Shah, A. Wahid, and H. Yu, "Green IoT: An investigation on energy saving practices for 2020 and beyond," *IEEE Access*, vol. 5, pp. 15667–15681, 2017.
- [12] V. Nkemeni, F. Mieyeville, G. S. Kuaban, P. Czekalski, K. Tokarz, W. B. Nsanyuy, E. M. D. Djomadji, M. L. Kathe, P. Tsafack, and B. Zieliński, "Evaluation of green strategies for prolonging the lifespan of linear wireless sensor networks," *Sensors*, vol. 24, no. 21, p. 7024, Oct. 2024.
- [13] A. Kansal, J. C. Hsu, S. Zahedi, and M. Srivastava, "Power management in energy harvesting sensor networks," *ACM Trans. Embedded Comput. Syst.*, vol. 6, no. 4, p. 32, Sep. 2007.

- [14] E. Gelenbe, "Energy packet networks: ICT based energy allocation and storage," in *Proc. Int. Conf. Green Commun. Netw.* Cham, Switzerland: Springer, Jan. 2012, pp. 186–195.
- [15] E. Gelenbe, "Energy packet networks: Adaptive energy management for the cloud," in *Proc. 2nd Int. Workshop Cloud Comput. Platforms*, Apr. 2012, pp. 1–5, doi: [10.1145/2168697.2168698](https://doi.org/10.1145/2168697.2168698).
- [16] G. S. Kuaban, T. Czachórski, E. Gelenbe, S. Sharma, and P. Czekalski, "A Markov model for a self-powered green IoT device with state-dependent energy consumption," in *Proc. 4th Int. Conf. Commun., Inf., Electron. Energy Syst. (CIEES)*, Nov. 2023, pp. 1–7.
- [17] A. Gautam and S. Dharmaraja, "An analytical model driven by fluid queue for battery life time of a user equipment in LTE-A networks," *Phys. Commun.*, vol. 30, pp. 213–219, Oct. 2018.
- [18] G. L. Jones, P. G. Harrison, U. Harder, and T. Field, "Fluid queue models of battery life," in *Proc. IEEE 19th Annu. Int. Symp. Modeling, Anal., Simulation Comput. Telecommun. Syst.*, Jul. 2011, pp. 278–285.
- [19] C. Tunc and N. Akar, "Markov fluid queue model of an energy harvesting IoT device with adaptive sensing," *Perform. Eval.*, vol. 111, pp. 1–16, May 2017.
- [20] O. H. Abdelrahman and E. Gelenbe, "A diffusion model for energy harvesting sensor nodes," in *Proc. IEEE 24th Int. Symp. Modeling, Anal. Simulation Comput. Telecommun. Syst. (MASCOTS)*, Sep. 2016, pp. 154–158.
- [21] T. Czachórski, E. Gelenbe, and G. S. Kuaban, "Modelling energy changes in the energy harvesting battery of an IoT device," in *Proc. 30th Int. Symp. Modeling, Anal., Simulation Comput. Telecommun. Syst. (MASCOTS)*. Nice, France: IEEE, Oct. 2022, pp. 81–88.
- [22] T. Czachórski, E. Gelenbe, G. S. Kuaban, and D. Marek, "Energy optimization for an unmanned aerial vehicle," in *Security in Computer and Information Sciences (Communications in Computer and Information Science)*, vol. 1596. Cham, Switzerland: Springer, 2022, pp. 61–75.
- [23] E. Gelenbe and Y. M. Kadioglu, "Battery attacks on sensors: Wireless nodes with battery attacks," in *Proc. Int. Symp. Comput. Inf. Sci., Cybersecur. Workshop*. Cham, Switzerland: Springer, Feb. 2018, pp. 61–75.
- [24] M. Raeis, A. Burchard, and J. Liebeherr, "Analysis of a queueing model for energy storage systems with self-discharge," *ACM Trans. Model. Perform. Eval. Comput. Syst.*, vol. 5, no. 3, pp. 1–26, Sep. 2020.
- [25] O. P. Angwech, A. S. Alfa, and B. T. J. Maharaj, "Managing the harvested energy in wireless sensor networks: A priority Geo/Geo/1/k approach with threshold," *Energy Rep.*, vol. 8, pp. 2448–2461, Nov. 2022.
- [26] D. Zhai, M. Sheng, X. Wang, and Y. Li, "Leakage-aware dynamic resource allocation in hybrid energy powered cellular networks," *IEEE Trans. Commun.*, vol. 63, no. 11, pp. 4591–4603, Nov. 2015.
- [27] N. Su and M. Koca, "Stochastic transmission policies for energy harvesting nodes with random energy leakage," in *Proc. 20th Eur. Wireless Conf.*, May 2014, pp. 1–6.
- [28] N. Dang, R. Valentini, E. Bozorgzadeh, M. Levorato, and N. Venkatasubramanian, "A unified stochastic model for energy management in solar-powered embedded systems," in *Proc. IEEE/ACM Int. Conf. Comput.-Aided Design (ICCAD)*, Nov. 2015, pp. 621–626.
- [29] J. Doncel and J.-M. Fourné, "Balancing energy consumption and losses with energy packet network models," in *Proc. IEEE Int. Conf. Fog Comput. (ICFC)*, Jun. 2019, pp. 59–68.
- [30] E. Gelenbe, "Minimizing delay and power consumption at the edge," *Sensors*, vol. 25, no. 2, p. 502, Jan. 2025, doi: [10.3390/s25020502](https://doi.org/10.3390/s25020502).
- [31] E. Gelenbe, "G-networks with instantaneous customer movement," *J. Appl. Probab.*, vol. 30, no. 3, pp. 742–748, Sep. 1993.
- [32] E. Gelenbe and Y. M. Kadioglu, "Energy loss through standby and leakage in energy harvesting wireless sensors," in *Proc. IEEE 20th Int. Workshop Comput. Aided Modeling Design Commun. Links Netw. (CAMAD)*, Sep. 2015, pp. 231–236.
- [33] Y. M. Kadioglu and E. Gelenbe, "Product-form solution for cascade networks with intermittent energy," *IEEE Syst. J.*, vol. 13, no. 1, pp. 918–927, Mar. 2019.
- [34] S. Zhang, A. Seyed, and B. Sikdar, "An analytical approach to the design of energy harvesting wireless sensor nodes," *IEEE Trans. Wireless Commun.*, vol. 12, no. 8, pp. 4010–4024, Aug. 2013.
- [35] A. Seyed and B. Sikdar, "Modeling and analysis of energy harvesting nodes in wireless sensor networks," in *Proc. 46th Annu. Allerton Conf. Commun., Control, Comput.*, Sep. 2008, pp. 67–71.
- [36] P. Lee, Z. A. Eu, M. Han, and H.-P. Tan, "Empirical modeling of a solar-powered energy harvesting wireless sensor node for time-slotted operation," in *Proc. IEEE Wireless Commun. Netw. Conf.*, Mar. 2011, pp. 179–184.
- [37] A. Jaitawat and A. K. Singh, "Battery and supercapacitor imperfections modeling and comparison for RF energy harvesting wireless sensor network," *Wireless Netw.*, vol. 26, no. 2, pp. 843–853, Feb. 2020.
- [38] D. G. Kendall, "Stochastic processes occurring in the theory of queues and their analysis by the method of the imbedded Markov chain," *Ann. Math. Statist.*, vol. 24, no. 3, pp. 338–354, Sep. 1953.
- [39] S. Samain, J. Doncel, A. Busic, and J.-M. Fourné, "Multiclass energy packet networks with finite capacity energy queues," *Perform. Eval.*, vol. 152, Dec. 2021, Art. no. 102228.
- [40] L. Kleinrock, *Queueing Systems, Volume 1: Theory*. Hoboken, NJ, USA: Wiley, 1975.
- [41] G. S. Kuaban, T. Czachórski, E. Gelenbe, P. Pecka, S. Sharma, P. Singh, V. Nkemeni, and P. Czekalski, "Energy performance of self-powered green IoT nodes," *Frontiers Energy Res.*, vol. 12, Nov. 2024, Art. no. 1399371.
- [42] P. Pecka, M. Nowak, A. Rataj, and S. Nowak, "Solving large Markov models described with standard programming language," in *Proc. Int. Symp. Comput. Inf. Sci.* Cham, Switzerland: Springer, 2018, pp. 57–67.
- [43] J. Ahn, D. Kim, R. Ha, and H. Cha, "State-of-Charge estimation of supercapacitors in transiently-powered sensor nodes," *IEEE Trans. Comput.-Aided Design Integr. Circuits Syst.*, vol. 41, no. 2, pp. 225–237, Feb. 2022.
- [44] G. V. Merrett, A. S. Weddell, A. P. Lewis, N. R. Harris, B. M. Al-Hashimi, and N. M. White, "An empirical energy model for supercapacitor powered wireless sensor nodes," in *Proc. 17th Int. Conf. Comput. Commun. Netw.*, Aug. 2008, pp. 1–6.
- [45] H. Yang and Y. Zhang, "Evaluation of supercapacitor models for wireless sensor network applications," in *Proc. 5th Int. Conf. Signal Process. Commun. Syst. (ICSPCS)*, Dec. 2011, pp. 1–6.
- [46] A. S. Weddell, G. V. Merrett, T. J. Kazmierski, and B. M. Al-Hashimi, "Accurate supercapacitor modeling for energy harvesting wireless sensor nodes," *IEEE Trans. Circuits Syst. II, Exp. Briefs*, vol. 58, no. 12, pp. 911–915, Dec. 2011.



GODLOVE SUILA KUABAN received the B.Eng. degree in electrical and electronics engineering, with a specialization in telecommunications from the University of Buea, Cameroon, in 2014, and the M.Sc. degree in inter-disciplinary studies of automatic control, robotics, electronics, telecommunications, and computer science and specialized in computer science and the Ph.D. degree in telecommunications and technical computer science from the Silesian University of Technology, Gliwice, Poland, in 2017 and 2023, respectively. From 2017 to 2023, he was a Research Assistant with the Institute of Theoretical and Applied Informatics, Polish Academy of Science (IITiS-PAN), Gliwice. He is currently an Assistant Professor with IITiS-PAN. His research interests include computer systems modelling and performance evaluations. Specifically, modeling and evaluations of software defined networking (SDN) and IoT networks and energy performance of green networks (e.g., IoT and cellular mobile networks and linear wireless sensor networks). He has participated in six EU-funded research grants: three in IoT security, one in building IoT laboratory testbed, one in developing online education resources on assembly language programming, and one on reliable electronics for tomorrow's active systems. Also, he received the Best Paper Award at the International Symposium on the Modelling, Analysis, and Simulation of Computer and Telecommunication Systems (MASCOTS 2023) in Stony Brook, NY, USA, and MASCOTS 2024 in Krakow, Poland (published by IEEE).



TADEUSZ CZACHÓRSKI (Member, IEEE) received the M.Sc., Ph.D., and D.Sc. degrees in informatics from the Silesian University of Technology, Gliwice, in 1972, 1979, and 1988, respectively. Since 1972, he has been a Researcher with the Institute of Theoretical and Applied Informatics of Polish Academy of Sciences (IITiS-PAN), Gliwice. He was a Professor, in 1999. He was for over two decades a Professor with the Silesian University of Technology and

also spent more than five years at several French universities and research institutes (IRISA Rennes, University of Versailles, ISEM Orsay Paris-Sud, Paris-Nord, and National Institute of Telecommunications) and still maintains scientific cooperation with some of them. From 1990 to 2007, he was the Scientific Secretary of the Committee of Informatics of Polish Academy of Sciences, between 2007 and 2011, he was the Vice-President of this Committee. He currently heads the Committee's Section of Computer Networks and Distributed Systems. He is also the Former Chair of IFIP Technical Committee TC5 "Information Technology and Applications" and a member of the IFIP General Assembly. His scientific research interests include mathematical methods and software related to modeling and performance evaluation of wide area computer networks, especially the internet. The methods include Markov chains, diffusion approximation and fluid flow approximation used to study quality of service, traffic control mechanisms, and related problems.



EROL GELENBE (Life Fellow, IEEE) received the B.S. degree in electrical and electronic engineering from Middle East Technical University, Ankara, in 1966, the master's and Ph.D. degrees from the Polytechnic Institute of Brooklyn (Tandon School of Engineering, New York University), in 1968 and 1970, respectively, the Doctor of Science (Habilitation) degree from Sorbonne University, Paris, in 1973, and the Polish Habilitation degree, in 2023. Known for his research contributions

to computer system and network performance evaluation, for developing diffusion approximations, inventing G-networks, and the random neural networks, he is also a fellow of ACM and IFIP. He is the co-author or author of four monographs in French and English, two of which were published in Japanese and Korean. He has graduated over 90 Ph.D.'s, including 24 women

and was awarded four Honorary Doctorates (Honoris Causa) from the University of Rome II, Bogaziçi University, Istanbul, University of Liège, Belgium, and Hungarian Academy of Sciences. He is a member of Academia Europaea, an elected Fellow of French National Academy of Technologies and Turkish Science Academy, a Foreign Fellow of the Science Academies of Belgium and Poland, and a Honorary Fellow of Hungarian Academy of Sciences and the Academy of Sciences of the Islamic World. He was awarded research prizes by the Parlar Foundation of Turkey, French Academy of Sciences, ACM, U.K.'s Institution for Engineering and Technology (IET), and the Mustafa Foundation.



PIOTR CZEKALSKI was born in Zabrze, Poland, in 1975. He received the B.S. and M.S. degrees in computer science and the Ph.D. degree from the Silesian University of Technology (SUT), in 1999 and 2004, respectively. He is currently working in parallel in several IT-related companies in Poland (including Computerland and Sygnity). He continues to work as an Assistant Professor with SUT. He is the author of many educational books and research articles and the Coordinator of

educational, research, and commercial research and development projects. His research interests include the Internet of Things, low-level programming techniques, and applied AI, particularly in the context of mobile and edge-class devices.

...